Wave function of $^9\mathrm{Be}$ in the three-body $(\alpha\alpha n)$-model

S. A. Rakityansky [a,b]

[a] Joint Institute for Nuclear Research, Dubna, Russia

[b] Department of Physics, University of Pretoria, Pretoria, South Africa

July 24, 2024

Abstract

A simple analytic expression of the three-body wave function describing the system $(\alpha\alpha n)$ in the ground state $\frac{3}{2}^-$ of $^9\mathrm{Be}$ is obtained. In doing this, it is assumed that the α particles interact with each other via the S-wave Ali-Bodmer potential including the Coulomb term, and the neutron-α forces act only in the P-wave state. This wave function is constructed by trial and error method via solving in this way a kind of inverse problem when the two-body $\alpha\alpha$ potential is recovered from a postulated three-body wave function. As a result, the wave function is an exact solution of the corresponding three-body Schrödinger equation for experimentally known binding energy and for the $\alpha\alpha$ potential whose difference from the Ali-Bodmer one is minimized by varying the adjustable parameters which the postulated wave function depends on.

1 Introduction

Beryllium isotope $^9\mathrm{Be}$ is of special interest from several points of view. First of all, it is clusterized with very high probability in two α particles and a neutron. As a result the low-lying spectrum of this nucleus is well-reproduced within the three-body $(\alpha\alpha n)$-model [1–5].

Secondly, neither $\alpha\alpha$ nor αn pairs can form bound states, which means that this isotope is an example of a Borromean system with a rather small binding energy of $1.5736\,\mathrm{MeV}$ [6].

Thirdly, due to such a weak three-body binding the valence neutron is loosely bound as well. This means that the neutron should move rather far away from the centre of mass, which makes the nucleus $^9\mathrm{Be}$ a transient one between ordinary compact nuclei and the halo-nuclei.

And finally, the last but not least is the fact that $^9\mathrm{Be}$ plays an important role in astrophysical processes, namely, in synthesis of heavy elements in the universe. Since there are no stable nuclei with $A = 5$ and $A = 8$, the two-body pp-chain reactions practically stop at the formation of $^4\mathrm{He}$ [7, 8]. The synthesis of more heavy elements requires a bridge over these so-called $A = 5, 8$ mass gaps. These gaps can be crossed over via the three-body fusion reactions. Among them the most well known is the triple-alpha fusion, $\alpha\alpha\alpha \to {}^{12}\mathrm{C} + \gamma$, which is usually associated with the Hoyle resonance (see, for example, Ref. [9]). In a neutron-rich environment one of the alternative bridges is provided by the radiative process $n(\alpha\alpha, \gamma)^9\mathrm{Be}$ which involves the Beryllium isotope that is considered in the present paper.

Of course, in addition to what was already said, the nucleus $^9\mathrm{Be}$ appears either in the initial or in the final states of various nuclear reactions, such as $^9\mathrm{Be}(n, \gamma)^{10}\mathrm{Be}$ [10], $^9\mathrm{Be}(^{18}\mathrm{O}, ^{17}\mathrm{O})^{10}\mathrm{Be}$ [11], $^8\mathrm{Li}(p, \gamma)^9\mathrm{Be}$ [12, 13], etc.

When theoretically describing the processes mentioned above, one usually needs the wave functions of the quantum systems involved, and in particular the wave function of $^9\mathrm{Be}$. There are many different approaches to obtaining such a function.

Strictly speaking, this nucleus should be considered as a nine-body system. Such an (ab initio) approach can be based either on the shell model or on the expansion over the hyperspherical harmonics. However, as was mentioned before, $^9\mathrm{Be}$ is clusterized in two α particles and a neutron. Thanks to the tight binding of $^4\mathrm{He}$ ($\sim 28\,\mathrm{MeV}$), the α particles move inside $^9\mathrm{Be}$ like solid bodies without internal excitations, and therefore the nine-body problem can be reduced to an effective three-body one. To the best of the author's knowledge all the calculations that were done for $^9\mathrm{Be}$ during the last few decades, exploited the $(\alpha\alpha n)$ cluster-representation. The three-body problem can also be solved in different ways: either using exact Faddeev equations (see, for example, Refs. [2, 3]), or with the help of various approximate methods [4, 14–16].

The common feature of all the publications, where these three-body approaches are realised, is that the wave function of $^9\mathrm{Be}$ is not given (and in most cases cannot be given) in such a form that could be used by the other people in their own calculations. In other words, if somebody wants to use the same wave function, he or she has to repeat all the complicated calculations described in these publications. However, for the majority of the researchers this is a difficult obstacle. Indeed, the procedure of solving, for example, the Faddeev equations involves many mathematical and numerical tricks that are only known to those who specialize in the field of the few-body problem. The shell model and the hyperspherical expansion are not much easier. It is therefore desirable to have some parametrized analytic expressions of the wave functions of various nuclei that are easy to use. This is what the present paper is devoted to. Here such a parametrization is obtained for the wave function of $^9\mathrm{Be}$ in the three-body cluster model $(\alpha\alpha n)$.

The way of obtaining the parametrized three-body wave function is based on the work by

Belyaev et al. [17]. That parer deals with a three-body problem in which two of the three pairwise potentials as well as the three-body wave function are given while one of the two-body potentials is unknown. The authors of Ref. [17] developed a method for recovering this unknown potential.

In the present work, this method is kind of "reversed", i.e. the wave function is postulated in a parametrized form and its parameters are optimized by minimizing the difference between the recovered potential and the corresponding exact one. For the system under consideration, $(\alpha\alpha n)$, it is chosen the $\alpha\alpha$ potential for the role of recovered one. The analytic form of the wave function and its parameters are chosen to fit (as close as possible) the Ali-Bodmer potential [18].

2 Formalism

Consider a bound state of two α particles and a neutron with a negative three-body energy E_b. It is known [6] that this system has only one bound state, which is the nucleus $^9\mathrm{Be}$. Using the Jacobi coordinates shown in Fig. 1, the three-body Schrödinger equation for the wave function $\Psi(\vec{r}_{\alpha\alpha}, \vec{r}_n)$ describing $^9\mathrm{Be}$, can be written as follows:

$$V_{\alpha\alpha}(r_{\alpha\alpha})\Psi(\vec{r}_{\alpha\alpha}, \vec{r}_n) = \tag{1}$$

$$= \left[E_b - V_{\alpha n}(\rho_1) - V_{\alpha n}(\rho_2) + \frac{\hbar^2}{2\mu_{\alpha\alpha}}\Delta_{\vec{r}_{\alpha\alpha}} + \frac{\hbar^2}{2\mu}\Delta_{\vec{r}_n}\right]\Psi(\vec{r}_{\alpha\alpha}, \vec{r}_n) \ ,$$

where $V_{\alpha\alpha}$ and $V_{\alpha n}$ are the two-body potentials for the $\alpha\alpha$ and αn pairs, $\mu_{\alpha\alpha} = m_\alpha/2$ and $\mu = 2m_\alpha m_n/(2m_\alpha + m_n)$ are the reduced masses corresponding to the respective Jacobi coordinates, the radial variables ρ_1 and ρ_2 given by

$$\rho_{1,2} = \sqrt{\frac{1}{4}r_{\alpha\alpha}^2 + r_n^2 \mp r_{\alpha\alpha}r_n\cos\vartheta} \ , \tag{2}$$

are the distances between the neutron the the α particles, and the Laplacians involve the derivatives with respect to the corresponding Jacobi vectors.

Multiplying Eq. (1) by $\Psi^\dagger(\vec{r}_{\alpha\alpha}, \vec{r}_n)$ from the left and integrating over vector $\vec{r}_n$ as well as over the spherical angles, $\Omega_{\alpha\alpha}$, of vector $\vec{r}_{\alpha\alpha}$, one can find the potential $V_{\alpha\alpha}$, if the energy E_b,

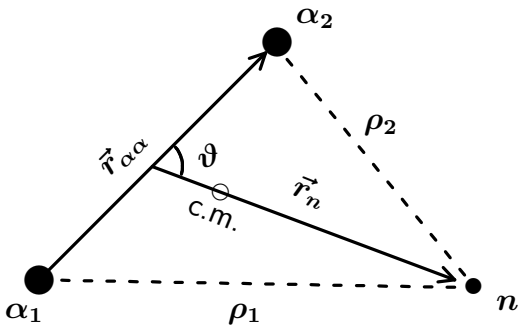

Figure 1: Jacobi coordinates, $\vec{r}_{\alpha\alpha}$ and $\vec{r}_n$, that specify a space configuration of the system $(\alpha\alpha n)$. The symbols ρ_1 and ρ_2 denote distances between the neutron and the two alpha particles.

the potential $V_{\alpha n}$, and the function $\Psi(\vec{r}_{\alpha\alpha}, \vec{r}_n)$ are given,

$$V_{\alpha\alpha}(r_{\alpha\alpha}) = E_b - \tag{3}$$

$$- \frac{1}{D(r_{\alpha\alpha})} \int d\Omega_{\alpha\alpha} d^3 r_n \Psi^\dagger(\vec{r}_{\alpha\alpha}, \vec{r}_n) \Big[V_{\alpha n}(\rho_1) + V_{\alpha n}(\rho_2) -$$

$$- \frac{\hbar^2}{2\mu_{\alpha\alpha}} \Delta_{\vec{r}_{\alpha\alpha}} - \frac{\hbar^2}{2\mu} \Delta_{\vec{r}_n} \Big] \Psi(\vec{r}_{\alpha\alpha}, \vec{r}_n) \ ,$$

where

$$D(r_{\alpha\alpha}) = \int d\Omega_{\alpha\alpha} d^3 r_n \Psi^\dagger(\vec{r}_{\alpha\alpha}, \vec{r}_n) \Psi(\vec{r}_{\alpha\alpha}, \vec{r}_n) \tag{4}$$

is the relative $\alpha\alpha$ radial probability density.

It should be noted that the wave function $\Psi(\vec{r}_{\alpha\alpha}, \vec{r}_n)$ is (by construction) the exact solution of the Schrödinger equation with a given E_b and with the potential $V_{\alpha\alpha}$ which is obtained from Eq. (3). This means that, if one chooses an approximate Ψ, it is still an exact solution of Eq. (1) with the corresponding approximate $V_{\alpha\alpha}$. The difference of this approximate $\alpha\alpha$ potential from the one, which is considered as the exact potential, characterizes the quality of the chosen Ψ. If one manages to find such a function Ψ that the potential, which follows from Eq. (3), is almost the same as the exact one, one actually finds a reliable solution of Eq. (1) for a given energy E_b. This can be achieved by varying the parameters of a postulated function Ψ in order to minimize the difference between the approximate and the exact $\alpha\alpha$ potentials.

3 Two-body potentials

The main input information that is needed in the present work is given by the $\alpha\alpha$ and αn two-body potentials. As is explained in the next section, these potentials are needed for the S-wave and P-wave states, respectively. The first of them is taken from Ref. [18]. This is well known Ali-Bodmer $\alpha\alpha$-potential:

$$V_{\alpha\alpha}(r) = V_R e^{-(\beta_R r)^2} - V_A e^{-(\beta_A r)^2} + V_c(r) \ , \tag{5}$$

which involves the repulsive and attractive Gaussian terms as well as the repulsive electric (Coulomb-like) one,

$$V_c(r) = \frac{4e^2}{r} \, \mathrm{erf}\left(\frac{\sqrt{3}}{2R_\alpha} r \right) \ . \tag{6}$$

The parameters of this potential are: $V_R = 1050\,\mathrm{MeV}$, $\beta_R = 0.8\,\mathrm{fm}^{-1}$, $V_A = 150\,\mathrm{MeV}$, $\beta_A = 0.5\,\mathrm{fm}^{-1}$, $R_\alpha = 1.44\,\mathrm{fm}$. The Coulomb term (6) takes into account a non-zero size of the α particle. The expression (6) is obtained under the assumption that its charge has a Gaussian distribution in space with the rms-radius R_α.

The αn potential in the present work is the same that was suggested by Bang and Gignoux [19]. It is of the Woods-Saxon type with a spin-orbit term:

$$V_{\alpha n}(r) = \frac{W_1}{1 + \exp\left[(r - R_1)/d_1\right]} + \frac{\vec{\ell} \cdot \vec{s}}{r} \frac{d}{dr} \frac{W_2}{1 + \exp\left[(r - R_2)/d_2\right]} \ , \tag{7}$$

where $W_1 = -43.0\,\mathrm{MeV}$, $R_1 = 2.0\,\mathrm{fm}$, $d_1 = 0.7\,\mathrm{fm}$, $W_2 = 40.0\,\mathrm{MeV} \cdot \mathrm{fm}^2$, $R_2 = 1.5\,\mathrm{fm}$, $d_2 = 0.35\,\mathrm{fm}$. For the quantum state with the total angular momentum $J = 3/2$, orbital angular momentum $\ell = 1$, and the neutron spin $s = 1/2$, the action of the operator $\vec{\ell} \cdot \vec{s}$ is equivalent to multiplication by $1/2$.

The potentials (5, 7) were used by many authors in a number of calculations within the three-body models of $^9\mathrm{Be}$ and $^6\mathrm{Li}$ (see, for example, Refs. [2, 3, 19] where the corresponding three-body Faddeev equations were solved). It turned out that these potentials reliably described the $\alpha\alpha$ and αn interactions at low energies as well as allowed one to well reproduce the binding energies and the other properties of the nuclei. The potentials (5, 7) are therefore used in the present paper as well.

4 Wave function of $^9\mathrm{Be}$

As was explained in the Introduction, the Beryllium isotope $^9\mathrm{Be}$ is clusterized in two α particles and a neutron. This is a Borromean three-body system that has only one bound state with

a rather small binding energy $|E_b| = 1.5736\,\mathrm{MeV}$ and with the spin-parity $(3/2)^-$ [6]. Since the α particle spins are zero, the three-body wave function should be symmetric with respect to the α-α permutation. This means that their relative orbital angular momentum is even, $\ell_{\alpha\alpha} = 0, 2, 4, \ldots$. The negative parity can therefore be obtained if the valence neutron moves with an odd orbital angular momentum, $\ell_n = 1, 3, 5, \ldots$, relative to the $\alpha\alpha$ pair.

As a reliable approximation, it is reasonable to assume that $\ell_{\alpha\alpha} = 0$ and $\ell_n = 1$. All the higher partial waves are ignored since the $(\alpha\alpha n)$ binding is weak and Borromean while high values of $\ell_{\alpha\alpha}$ and ℓ_n introduce additional repulsive centrifugal potentials into the three-body hamiltonianian. The minimal repulsion is in the state $\ell_{\alpha\alpha} = 0$, $\ell_n = 1$.

One may wonder why $\ell_n = 1$ and not zero, which would generate even less repulsion. An intuitive explanation can be found by considering the naive shell model as follows. There are five neutrons in this nucleus. Four of them are sitting in the clusters. Each cluster has its own mean-field potential and its own level structure. Two neutrons in the first α particle occupy its lowest S-level and the other two neutrons occupy the lowest S-level in the second α particle. What remains for the fifth neutron is the P-level either in the first or in the second cluster. Therefore the valence neutron moves in the P-wave state with respect to both α particles. This is therefore the shell-model configuration with the minimal energy. And since $\ell_{\alpha\alpha} = 0$, the orbital angular momentum of the neutron with respect of the centre of mass of the $\alpha\alpha$ subsystem is also one, i.e. $\ell_n = 1$.

Based on the above reasoning, one comes to the following structure of the wave function of ^{9}Be:

$$\Psi(\vec{r}_{\alpha\alpha}, \vec{r}_n) = R(r_{\alpha\alpha}, r_n) Y_{00}(\Omega_{\alpha\alpha}) \mathcal{Y}^{\frac{3}{2} J_z}_{1\frac{1}{2}}(\Omega_n) \ , \tag{8}$$

where the spin-angular function of the neutron, $\mathcal{Y}^{\frac{3}{2} J_z}_{1\frac{1}{2}}(\Omega_n)$, defined as

$$\mathcal{Y}^{JJ_z}_{\ell s}(\Omega) = \sum_{m s_z} C^{JJ_z}_{\ell m s s_z} Y_{\ell m}(\Omega) \chi_s(s_z) \ , \tag{9}$$

couples its orbital angular momentum and the spin. Here χ_s is the spin function of the neutron.

Substituting wave function (8) in Eqs. (3) and (4), the following decomposition of the $\alpha\alpha$ potential is obtained:

$$V_{\alpha\alpha}(r_{\alpha\alpha}) = E_b - \left\langle V_{\alpha n}(\rho_1) \ + V_{\alpha n}(\rho_2) \right\rangle - \left\langle \frac{\ell_n(\ell_n+1)}{r_n^2} \right\rangle + \langle E_{\mathrm{kin}} \rangle \ , \tag{10}$$

where the averaging, denoted by the brackets $\langle\rangle$, is done over all the configuration space variables except the radial variable $r_{\alpha\alpha}$. These average values represent the contributions that are originated from the two αn potentials,

$$\left\langle V_{\alpha n}(\rho_{1,2}) \right\rangle = \frac{3}{4D(r_{\alpha\alpha})} \int_0^\infty dr_n \int_0^\pi d\vartheta \, r_n^2 (\sin\vartheta)^3 V_{\alpha n}(\rho_{1,2}) \, |R(r_{\alpha\alpha}, r_n)|^2 \ , \tag{11}$$

from the centrifugal potential caused by $\ell_n = 1$,

$$\left\langle \frac{\ell_n(\ell_n+1)}{r_n^2} \right\rangle = \frac{\hbar^2}{\mu D(r_{\alpha\alpha})} \int_0^\infty dr_n \, |R(r_{\alpha\alpha}, r_n)|^2 \ , \tag{12}$$

and from the radial derivatives ("kinetic energy" terms) of the Laplacians $\Delta_{\vec{r}_{\alpha\alpha}}$ and $\Delta_{\vec{r}_n}$,

$$\begin{aligned} \langle E_{\rm kin} \rangle &= \frac{\hbar^2}{2\mu_{\alpha\alpha} r_{\alpha\alpha}^2 D(r_{\alpha\alpha})} \int_0^\infty dr_n \, r_n^2 R^*(r_{\alpha\alpha}, r_n) \frac{\partial}{\partial r_{\alpha\alpha}} \left[r_{\alpha\alpha}^2 \frac{\partial}{\partial r_{\alpha\alpha}} R(r_{\alpha\alpha}, r_n) \right] \\ &+ \frac{\hbar^2}{2\mu D(r_{\alpha\alpha})} \int_0^\infty dr_n \, R^*(r_{\alpha\alpha}, r_n) \frac{\partial}{\partial r_n} \left[r_n^2 \frac{\partial}{\partial r_n} R(r_{\alpha\alpha}, r_n) \right] \ , \end{aligned} \tag{13}$$

where

$$D(r_{\alpha\alpha}) = \int_0^\infty dr_n \, r_n^2 \, |R(r_{\alpha\alpha}, r_n)|^2 \ . \tag{14}$$

When obtaining Eq. (11) it was used the fact that the left hand side of Eq. (10) cannot depend on J_z. The simplest choice is $J_z = 3/2$ which implies that the sum in Eq. (9) only includes one term involving the spherical harmonics $Y_{11}(\vartheta, \varphi) = -(1/2)\sqrt{3/(2\pi)} \sin\vartheta \exp(i\varphi)$, where the z-axis is chosen along $\vec{r}_{\alpha\alpha}$ and the polar angle ϑ is between vectors $\vec{r}_{\alpha\alpha}$ and $\vec{r}_n$ (see Fig. 1).

It should be noted that in Eqs. (11-13) the normalization of the radial wave function $R(r_{\alpha\alpha}, r_n)$ is arbitrary. This is because in each of these equations the square of R is present in both the numerator and denominator. This fact significantly simplifies the procedure for fitting the potential $V_{\alpha\alpha}(r_{\alpha\alpha})$, because one does not have to care about proper nomalization of $R(r_{\alpha\alpha}, r_n)$ when varying its parameters. The function $R(r_{\alpha\alpha}, r_n)$ only needs to be normalized to unity at the final stage when all its parameters have been optimized and established.

The choice of a functional form of $R(r_{\alpha\alpha}, r_n)$ is the most important and difficult part of the described procedure. It was done by trial and error approach. After many unsuccessful attempts, it was found such a form of this radial wave function that Eq. (10) produced the potential curve whose shape was more or less similar to the Ali-Bodmer potential. Finally, the parameters of $R(r_{\alpha\alpha}, r_n)$ were adjusted by minimizing the difference between the Ali-Bodmer potential and the one produced by Eq. (10). This was done via the least-square method using the minimization code MINUIT [21].

The resulting radial wave function of ^{9}Be looks as follows:

$$R(r_{\alpha\alpha}, r_n) = \frac{N}{r_{\alpha\alpha}^2 r_n^3} \arctan\left[(a_1 r_{\alpha\alpha})^{7/2}\right] \arctan\left[(a_2 r_n)^{7/2}\right] \left[1 - e^{-(a_3 r_{\alpha\alpha})^2}\right]^2 \frac{e^{-\varkappa\zeta}}{\zeta^{5/2}} \ , \tag{15}$$

where $\varkappa = \sqrt{2\mu|E_b|/\hbar^2}$ is the momentum corresponding to the experimental binding energy,

$$\zeta = \sqrt{\frac{\mu_{\alpha\alpha}}{\mu} r_{\alpha\alpha}^2 + r_n^2} \tag{16}$$

is the hyperradius, $a_1 = 0.37441\,\mathrm{fm}^{-1}$, $a_2 = 0.070112\,\mathrm{fm}^{-1}$, $a_3 = 0.41953\,\mathrm{fm}^{-1}$, and the normalization constant $N = 927446.734\,\mathrm{fm}^{9/2}$.

A specific choice of the functional form of $R(r_{\alpha\alpha}, r_n)$ was based on some general properties of such a function as well as on the author's intuition. Unfortunately, there is no universal recipe for constructing this function.

The following general features of the wave function were taken into account. First of all, the radial wave function must exponentially tend to zero at large distances in all directions in the configuration space. It is known from the hyperspherical expansion theory that for any three-body system such an exponential diminishing is given by the factor $e^{-\varkappa\zeta}/\zeta^{5/2}$. This is why this factor is present in the expression (15). Due to the Pauli blocking, the α particles cannot penetrate each other. For the same reason the neutron cannot move inside them. Therefore the Pauli blocking requires vanishing of the wave function when $r_{\alpha\alpha}$ and r_n tend to zero. And finally, the wave function should have maxima at some short distances along both radial variables, $r_{\alpha\alpha}$ and r_n. These maxima correspond to the most probable configuration of the system.

A maximum at some intermediate distance along the variable x as well as vanishing near $x = 0$ can be implemented by using the function $\arctan[(ax)^n]/x^m$ with $n > m$. There are two such factors in the function (15), for $x = r_{\alpha\alpha}$ and for $x = r_n$. In principle, the powers n and m could be made additional adjustable parameters. However, it was decided not to increase the number of the free parameters, because a multi-variable function usually has many local minima and threfore with too many variable parameters the fitting of the potential could be more difficult. The optimal values of n and m for the variables $r_{\alpha\alpha}$ and r_n were found manually by the trial and error method.

It turned out that the suppression of $R(r_{\alpha\alpha}, r_n)$ at $r_{\alpha\alpha} \to 0$ that was provided by the corresponding factor $\sim \arctan(.)$, was insufficient (the resulting $V_{\alpha\alpha}$ potential was too soft at the origin). In order to increase the suppression, an additional factor $[1 - e^{-(a_3 r_{\alpha\alpha})^2}]^2$ was introduced.

The wave function (8) with the radial part (15) is an exact solution of Eq. (3) for the $\alpha\alpha$ potential shown in Fig. (2) by the solid curve. As is seen, this reconstructed potential is very close to the Ali-Bodmer one. On one hand it is a bit different, but on the other hand it corresponds to the exact experimental binding energy of $^9\mathrm{Be}$.

In order to check how good the reconstructed potential is in describing the low-energy $\alpha\alpha$ scattering, the S-wave scattering phase shifts were calculated and compared with the corresponding values for the Ali-Bodmer potential. For obtaining the phase shifts the differential equations for the Jost functions were numerically integrated (see Eqs. (8.57, 8.58) of the book [22]). The results of these calculations are shown in Fig. 3, where the solid curve corresponds to the reconstructed potential while the dashed curve represents the Ali-Bodmer one. In Fig. 3 these phase shifts are compared not only with each other but also with the corre-

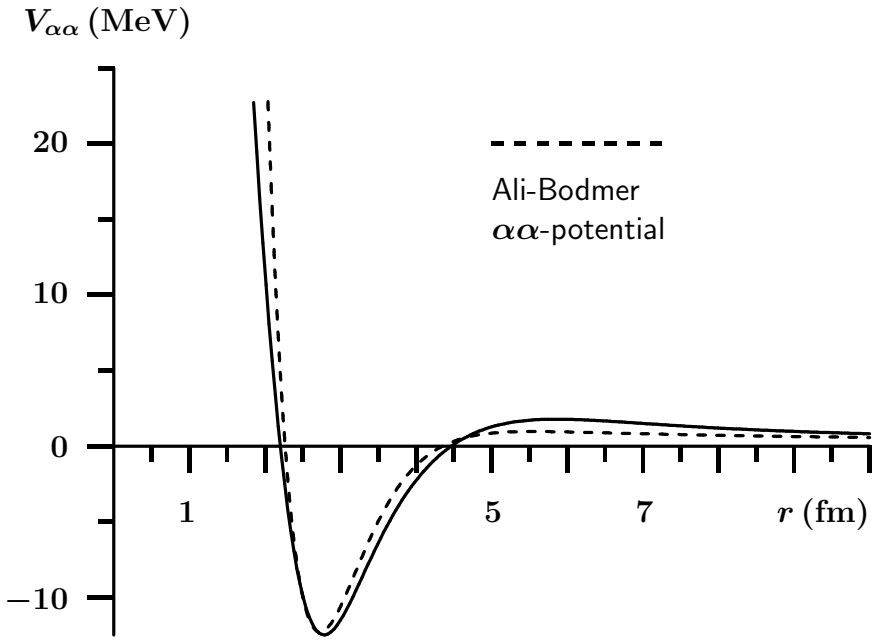

Figure 2: The exact Ali-Bodmer potential (5) shown by the dashed curve, and the $\alpha\alpha$ potential corresponding to the wave function (8) with the radial part (15) (solid curve).

sponding experimental values. The experimental data are available (see Refs. [23, 24]) as the so-called nuclear parts of the phase shifts, i.e. the pure Coulomb phase shifts are subtracted. In calculating the curves such a subtraction was done as well.

The purpose of this comparison is to indirectly check the quality of the wave function (8) with the radial part (15). Since the reconstructed potential is not very much different from the Ali-Bodmer one and since it generates almost the same phase shifts that are also close to experimental data, one can say that in a possible application of this wave function it can be considered as a reliable approximation of the exact solution of the three-body Schrödinger equation (1) with the two-body potentials given in Sec. 3.

An additional test of the wave function that is obtained in the present work can be done by calculating various space-distances in the bound $(\alpha\alpha n)$ state which this wave function describes. It should be emphasized that none of the root-mean-square (RMS) distances that are calculated and given in Table 1, were fitted. The fit (by varying the parameters a_1, a_2, and a_3) was only done for the $\alpha\alpha$ potential. The RMS distances are just those that the resulting wave function gives.

The calculation of the RMS distances is reduced to one- or three-dimensional integrals

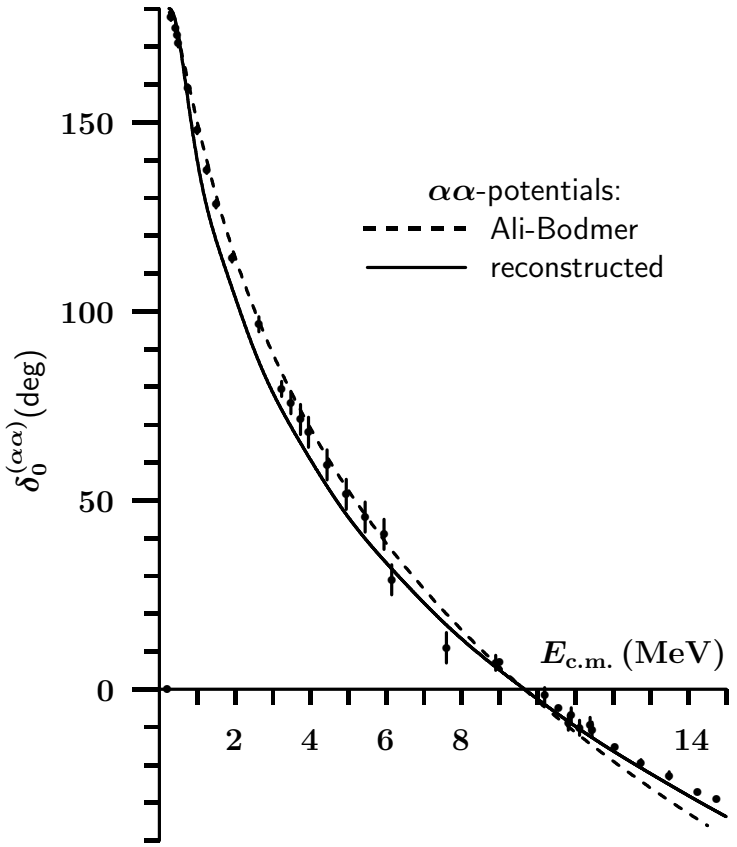

Figure 3: The S-wave phase shift for the Ali-Bodmer potential (5) shown by the dashed curve, and the corresponding phase shift for the $\alpha\alpha$ potential reconstructed from the wave function (8) with the radial part (15) (solid curve). The experimental data are taken from Refs. [23, 24].

over $r_{\alpha\alpha}$, r_n, and ϑ (see Fig. 1):

$$\langle r^2_{\alpha\alpha}\rangle = \left\langle \Psi \left| r^2_{\alpha\alpha} \right| \Psi \right\rangle \ , \tag{17}$$

$$\langle r^2_{{\rm cm}-n}\rangle = \left\langle \Psi \left| \left(\frac{2m_\alpha}{2m_\alpha + m_n} r_n \right)^2 \right| \Psi \right\rangle \ , \tag{18}$$

$$\langle r^2_{{\rm cm}-\alpha}\rangle = \left\langle \Psi \left| \left(\frac{1}{2}\vec{r}_{\alpha\alpha} - \frac{m_n}{2m_\alpha + m_n}\vec{r}_n \right)^2 \right| \Psi \right\rangle \ . \tag{19}$$

When finding the RMS charge and matter radii of ^{9}Be, the corresponding non-zero radii of the α particle, $R_{\mathrm{ch}(\alpha)} = 1.67824\,\mathrm{fm}$ [25] and $R_{\mathrm{mat}(\alpha)} = 1.457\,\mathrm{fm}$ [26] should be taken into account:

$$\langle r^2_{\mathrm{ch}}\rangle = \langle r^2_{\mathrm{cm}-\alpha}\rangle + R^2_{\mathrm{ch}(\alpha)}\ , \tag{20}$$

$$\langle r^2_{\mathrm{mat}}\rangle = \frac{2m_\alpha}{2m_\alpha + m_n}\left[\langle r^2_{\mathrm{cm}-\alpha}\rangle + R^2_{\mathrm{mat}(\alpha)}\right] + \frac{m_n}{2m_\alpha + m_n}\langle r^2_{\mathrm{cm}-n}\rangle\ . \tag{21}$$

distance	calculated (fm)	measured (fm)
$\sqrt{\langle r^2_{\alpha\alpha}\rangle}$	3.46	
$\sqrt{\langle r^2_{\mathrm{cm}-n}\rangle}$	4.65	
$\sqrt{\langle r^2_{\mathrm{cm}-\alpha}\rangle}$	1.83	
$\sqrt{\langle r^2_{\mathrm{ch}}\rangle}$	2.48	2.519 [27, 28]
$\sqrt{\langle r^2_{\mathrm{mat}}\rangle}$	2.70	2.50 ± 0.01 [29]

Table 1: Various RMS distances in ^{9}Be: between the α particles ($\sqrt{\langle r^2_{\alpha\alpha}\rangle}$), from c.m. to the valence neutron ($\sqrt{\langle r^2_{\mathrm{cm}-n}\rangle}$), from c.m. to the α particle ($\sqrt{\langle r^2_{\mathrm{cm}-\alpha}\rangle}$), charge radius of the nucleus ($\sqrt{\langle r^2_{\mathrm{ch}}\rangle}$), matter radius of the nucleus ($\sqrt{\langle r^2_{\mathrm{mat}}\rangle}$). The experimental data are taken from Refs. [27–29].

As is seen, the charge radius, $\sqrt{\langle r^2_{\mathrm{ch}}\rangle}$, turned out to be very close to the corresponding experimental value. The matter radius, $\sqrt{\langle r^2_{\mathrm{mat}}\rangle}$, is a bit too large as compared to the measurement. The difference, however, is not drastic. A very close result, namely, the value of 2.68 fm for the matter radius of ^{9}Be was obtained in Ref. [30] within the three-body model with microscopic nonlocal interactions based on Volkov V2 potential. Also, it should be noted that in contrast to a rather simple and accurate procedure for experimental determination of the charge radius, the measurements of the matter radii of the nuclei are always more difficult and are not without some ambiguities [26].

A quasi-3D image of the radial part (15) of the wave function of ^{9}Be is given in Fig. 4. This function has a maximum at $r_{\alpha\alpha} = 2.4051\,\mathrm{fm}$ and $r_n = 1.4654\,\mathrm{fm}$. It is also clearly seen a "ridge" along r_n with $r_{\alpha\alpha} \sim 2\,\mathrm{fm}$. This extended "ridge" is the cause of rather large values of $\sqrt{\langle r^2_{\mathrm{cm}-n}\rangle}$ and $\sqrt{\langle r^2_{\mathrm{mat}}\rangle}$.

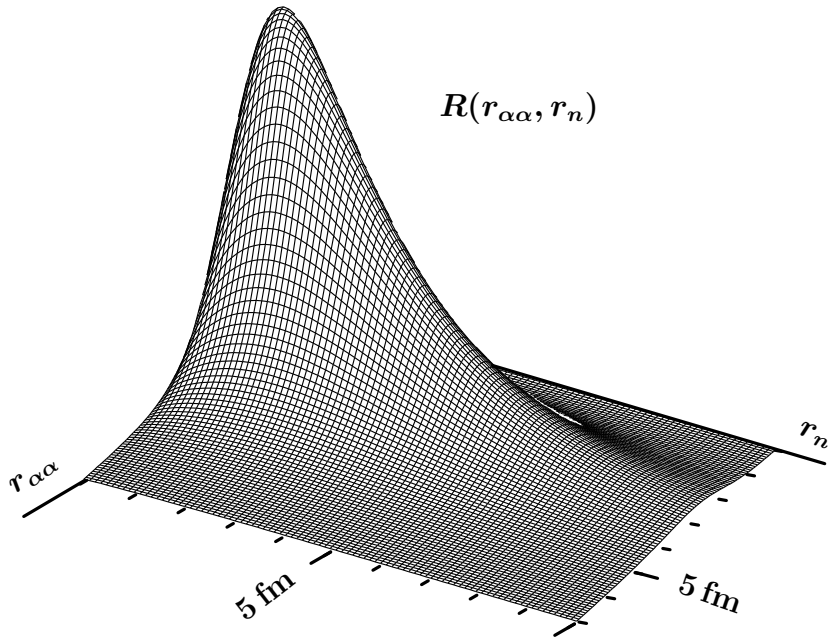

Figure 4: Radial part (15) of the wave function of $^9\mathrm{Be}$.

5 Conclusion

The wave function (8) with the radial part (15) is an exact bound-state solution of the three-body integro-differential equation (3) which follows from the equivalent Schrödinger equation (1). By construction, this solution corresponds to the experimentally known binding energy, as well as to the αn potential (7), and to the $\alpha\alpha$ potential that is almost the same as the Ali-Bodmer one. It can therefore be considered as a reliable approximation of the wave function of the nucleus $^9\mathrm{Be}$ in the three-body model ($\alpha\alpha n$).

This wave function is obtained in the form of a compact analytical expression that is easy to use. Among possible applications of this function could be, for example, the constructing of various folding potentials as well as estimating the cross sections of various nuclear reactions that involve $^9\mathrm{Be}$.

The method used in the present paper, is universal and can be applied for constructing the ground-state wave functions of any other nuclear or some atomic bound three-body systems. Of course it cannot compete with the approaches based on Faddeev equations, hyperspherical expansions, etc., where whole spectrum of the excited states can be described. However, the proposed method has its own application niche where it may be preferable. In particular, this method is suitable for the systems that have no excited states, such as, for example, the

nucleui $^6\mathrm{He}$ and $^6\mathrm{Li}$ if they are considered in the three-body model (αNN). The proposed method can give an analytical expression for the wave function which is easy to use when one needs a reliable estimate of something and does not want to delve into complicated numerical calculations of the rigorous three-body theory. In principle, the excited state wave functions can be constructed within this method as well. This, however, will require additional effort in making the excited states orthogonal to the ground state and to each other.

The method can be generalized for constructing the wave functions that are linear combinations of several mutually orthogonal components. For example, the ground 0^+-state of $^6\mathrm{He}$ in the (αnn)-model is mainly composed of the two components: the state $|\Psi_0\rangle$ with zero nn-spin as well as zero orbital angular momenta associated with both nn and $\alpha(nn)$ Jacobi coordinates (82.87%), plus the state $|\Psi_1\rangle$ with the nn-spin one and the P-waves along both Jacobi coordinates (13.96%) [31], i.e. $|\Psi\rangle = C_0|\Psi_0\rangle + C_1|\Psi_1\rangle$. In such a case, when going from Eq. (1) (which should be written for the nn-potential) to Eq. (3), one should multiply Eq. (1) from the left either by $\Psi_0^\dagger$ or by $\Psi_1^\dagger$ and integrate over all the configuration-space variables except the nn-distance. As a result one obtains a system of two coupled integro-differential equations where on the left hand sides are the singlet $(^1S_0)$ and triplet $(^3P_1)$ nn-potentials which can be fitted by adjusting the parameters of some postulated Ψ_0 and Ψ_1.

Another possible generalization of the proposed method may consist in considering four-, five-, and larger numbers of bodies in the bound system. In doing this, one term of the Schrödinger equation that involves a chosen two-body potential, can be moved to the left-hand side as is done in Eq. (1). Then whole equation should be multiplied from the left by $\Psi^\dagger$ and integrated over all the variables except the one which the chosen potential depends on. After that the wave function should be postulated and its parameters be adjusted in order to fit the potential. The main difficulty here is that with increasing number of particles it is not a simple task to find (to guess) an appropriate parametrization of the wave function because it depends on many variables. Moreover, even if one manages to find such a parametrization, the right-hand side of Eq. (3) will involve multi-dimensional integrals which may cause some numerical difficulties when the system under consideration consists of too many particles.

References

[1] Y.C. Tang, F.C. Khanna, R.C. Herndon, K. Wildermuth, "Be^9 in the cluster model", Nucl. Phys., **35**, 421-433 (1962)

[2] V.D. Efros, H. Oberhummer, A. Pushkin, I.J. Thompson, "Low-energy photodisintegration of $^9\mathrm{Be}$ and $\alpha+\alpha+n \leftrightarrow {}^9\mathrm{Be}+\gamma$ reactions at astrophysical conditions", The European

Physical Journal A - Hadrons and Nuclei, $\mathbf{1(4)}$, 447-453 (1998)
doi:10.1007/s100500050079

[3] I. Filikhin, V.M. Suslov, B. Vlahovic, "Be^9 Low-Lying Spectrum Within a Three-Cluster Model, Few-Body Syst., $\mathbf{50}$, 255-257 (2011)
https://doi.org/10.1007/s00601-010-0135-3

[4] J. Casal, M. Rodrıiguez-Gallardo, J.M. Arias, and I.J. Thompson, "Astrophysical reaction rate for $^9\mathrm{Be}$ formation within a three-body approach", Phys.Rev. C, $\mathbf{90}$, 044304 (2014)
DOI: 10.1103/PhysRevC.90.044304

[5] Elena Filandri, Paolo Andreatta, Carlo A. Manzata, Chen Ji, W. Leidemann, and G. Orlandini, "Beryllium-9 in Cluster Effective Field Theory", arXiv:2002.00780v1 [nucl-th] (2020)

[6] D.R. Tilley, J.H. Kelley, J.L. Godwin, D.J. Millener, J.E. Purcell, C.G. Sheu, and H.R. Weller, "Energy levels of light nuclei A $= 8, 9, 10$", Nucl. Phys., A $\mathbf{745}$, 155-362 (2004)

[7] Claus E. Rolfs and William S. Rodney, "Cauldrons in the Cosmos", The University of Chicago Press (1988)

[8] A. Aprahamian, K. Langanke, and M. Wiescher, "Nuclear structure aspects in nuclear astrophysics", Prog. Part. Nucl. Phys., $\mathbf{54}$, 535-613 (2005)

[9] Dr. Md A Khan, "Nuclear Astrophysics - A Course of Lectures", CRC Press, Taylor & Francis Group, International Standard Book Number-13: 978-1-138-58816-5, (2018)

[10] Peter Mohr, "Direct capture cross section of $^9\mathrm{Be}(n,\gamma)^{10}\mathrm{Be}$", Phys. Rev. C, $\mathbf{99}$, 055807 (2019)

[11] D. Carbone, M. Bondi, A. Bonaccorso, C. Agodi, F. Cappuzzello, M. Cavallaro, R. J. Charity, A. Cunsolo, M. De Napoli, and A. Foti, "First application of the $n - {}^9\mathrm{Be}$ optical potential to the study of the $^{10}\mathrm{Be}$ continuum via the $(^{18}\mathrm{O}, ^{17}\mathrm{O})$ neutron-transfer reaction", Phys. Rev. C, $\mathbf{90}$, 064621 (2014)

[12] Su Jun, Li Zhi-Hong, Guo Bing, Liu Wei-Ping, Bai Xi-Xiang, Zeng Sheng, Lian Gang, Yan Sheng-Quan, Wang Bao-Xiang, and Wang You-Bao, "Astrophysical Reaction Rates of the $^8\mathrm{Li}(p,\gamma)^9\mathrm{Be}_{\mathrm{g.}s.}$ Direct Capture Reaction", Chinese Physics Letters, $\mathbf{23\ (1)}$, 55-57 (2006)

[13] S.B. Dubovichenko, N.A. Burkova, A.V. Dzhazairov-Kakhramanov, "The role of resonances in the capture of $^{8}\mathrm{Li}(p,\gamma)^{9}\mathrm{Be}$ on the reaction rate of the relevant astrophysical synthesis of $^{9}\mathrm{Be}$", Nucl. Phys. A, $\mathbf{1000}$,121842 (2020) https://doi.org/10.1016/j.nuclphysa.2020.121842

[14] N. Itagaki, and K. Hagino, "Low-energy photodisintegration of $^{9}\mathrm{Be}$ with the molecular orbit model", Phys. Rev. C, $\mathbf{66}$, 057301 (2002)

[15] P. Descouvemont, T. Druet, L.F. Canto, M.S. Hussein, "Low-energy $^{9}\mathrm{Be} + {}^{208}\mathrm{Pb}$ scattering, breakup, and fusion within a four-body model", Phys. Rev. C, $\mathbf{91}$, 024606 (2015) DOI: 10.1103/PhysRevC.91.024606

[16] P. Descouvemont, and N. Itagaki, "$^{9}\mathrm{Be}$ scattering with microscopic wave functions and the continuum-discretized coupled-channel method", Phys. Rev. C, $\mathbf{97}$, 014612 (2018) DOI: 10.1103/PhysRevC.97.014612

[17] V.B. Belyaev, S.A. Rakityansky, I.M. Gopane, "Recovering the Two-Body Potential from a Given Three-Body Wave Function", Few-Body Syst., $\mathbf{64}$, 4 (2023) https://doi.org/10.1007/s00601-022-01785-7

[18] S. Ali and A.R. Bodmer, "PHENOMENOLOGICAL alpha-alpha POTENTIALS", Nucl.Phys.,$\mathbf{80}$, 99-112 (1966)

[19] J. Bang, C. Gignoux, "A REALISTIC THREE-BODY MODEL OF $^{6}\mathrm{Li}$ WITH LOCAL INTERACTIONS", Nucl. Phys. A, $\mathbf{313}$, 119-140 (1979)

[20] I.J. Thompson, B.V. Danilin, V.D. Efros, J.S. Vaagen, J.M. Bang, M.V. Zhukov, "Pauli blocking in three-body models of halo nuclei", Phys.Rev. C, $\mathbf{61}$ 024318 (2000)

[21] F. James and M. Roos, "Minuit - a system for function minimization and analysis of the parameter errors and correlations", Comp. Phys. Comm. 10 (1975) 343-367; http://hep.fi.infn.it/minuit.pdf

[22] S. A. Rakitiansky, "Jost Functions in Quantum Mechanics: A Unified Approach to Scattering, Bound, and Resonant State Problems", Springer (2022)

[23] S.A. Afzal, A.A.Z. Ahmad, S. Ali, "Systematic Survey of the α-α Interaction", Rev. Mod. Phys., $\mathbf{41}$(1), 247-273 (1969)

[24] W.S. Chien and Ronald E. Brown, "Study of the α+α system below 15 MeV (c.m.)", Phys. Rev. $\mathbf{C10}$(5), 1767-1784 (1974)

[25] Wilfried Nortershauser, "Helium nucleus measured with record precision", Nature, **589**, 518-519 (2021)

[26] I. Tanihata, H. Savajols, R. Kanungo, "Recent experimental progress in nuclear halo structure studies", Progress in Particle and Nuclear Physics, **68**,215-313 (2013)

[27] I. Angeli, K.P. Marinova, "Table of experimental nuclear ground state charge radii: An update", At. Data and Nucl. Data Tables, **99**(1), 69-95 (2013)
https://doi.org/10.1016/j.adt.2011.12.006

[28] Tao Li, Yani Luo, Ning Wang, "Compilation of recent nuclear ground state charge radius measurements and tests for models", At. Data and Nucl. Data Tables, **140**, 101440 (2021)
https://doi.org/10.1016/j.adt.2021.101440

[29] I. Tanihata, H. Hamagaki, O. Hashimoto, Y. Shida, and N. Yoshikawa, "Measurements of Interaction Cross Sections and Nuclear Radii in the Light p-Shell Region", Phys.Rev.Lett., **55**(24), 2676-2679 (1985)

[30] M. Theeten, H. Matsumura, M. Orabi, D. Baye, P. Descouvemont, Y. Fujiwara, and Y. Suzuki, "Three-body model of light nuclei with microscopic nonlocal interactions", Phys. Rev., **C76**, 054003 (2007)

[31] B.V. Danilin and M.V. Zhukov, S.N. Ershov, F.A. Gareev, and R.S. Kurmanov, J.S. Vaagen, J.M. Bang, "Dynamical multicluster model for electroweak and charge-exchange reactions", Phys. Rev., **C43**(6), pp. 2835-2843 (1991)